BRPF1 is essential for development of fetal hematopoietic stem cells

Linya You[1,2,§], Lin Li[1,2,§], Jinfeng Zou[3], Kezhi Yan[1,2], Jad Belle[4], Anastasia Nijnik[4,#], Edwin Wang[3,#] and Xiang-Jiao Yang[1,2,5,6,*]

[1]Rosalind & Morris Goodman Cancer Research Center and [2]Department of Medicine, McGill University, Montreal, Quebec H3A 1A3, Canada

[3]National Research Council Canada, Montreal, Quebec H4P 2R2, Canada

[4]Department of Physiology, McGill University, Montreal, Quebec H3A 1A3, Canada

[5]Department of Biochemistry, McGill University, and [6]McGill University Health Center, Montreal, Quebec H3A 1A3, Canada

[§]Co-first authors; [#]authors who made equal contribution.

[*]Goodman Cancer Center, Room 413, 1160 Pine Avenue West, Montreal, Quebec H3A 1A3, Canada; Tel: 514-398-5883; Email: xiang-jiao.yang@mcgill.ca

SUPPLEMENTARY INFORMATION

SUPPLEMENTAL EXPERIMENTAL PROCEDURES

Histological analysis. Femur and tibia were collected from control and vKO pups. The long bones were fixed in 4% paraformaldehyde and embedded in paraffin, and 5 μm sections were prepared on a Microtome (Leica, RM2125 RTS). Paraffin sections were dewaxed and stained with hematoxylin and eosin for histological examination as described (1, 2). Giemsa staining of either paraffin sections or bone marrow smear preparations was performed according to a procedure provided by Sigma-Aldrich.

Blood colony formation assays. Cells were harvested from the bone marrows of control and vKO pups or the fetal livers of control and vKO embryos. The cells were filtered through 40 μm cell strainers (StemCell Technologies) to obtain single-cell suspension, and red blood cells were lysed with an RBC lysis buffer (eBioscience). $6x10^4$ cells were cultured in Methocult M3434 (StemCell Technologies), and BFU-E, CFU-GM, CFU-GEMM colonies were enumerated on days 8-10. $1.5x10^5$ cells were cultured in Methocult M3630 (StemCell Technologies) to assess B cell colony formation on days 8-10.

Ki67 and Hoechst staining. Cells were harvested from the bone marrow of control and vKO pups or the fetal liver of control and vKO embryos, for staining with conjugated monoclonal antibodies (Table S5) as described in the main text to label HSCs and hematopoietic progenitors. Cells were fixed, permeabilized with the

Foxp3/transcription factor-staining buffer (eBioscience, Table S5), stained with Ki67-FITC (eBioscience) and analyzed with an LSR II flow cytometer (BD Biosciences).

For cell cycle analysis, fetal liver cells were stained with 10 μg/ml Hoechst 33342 in DMEM supplemented with 10% FBS and incubated at 37°C for 30 min. After a single wash, fetal liver cells were stained for surface markers of LSK cells and analyzed with the BD LSR II flow cytometer (BD Biosciences).

Annexin V staining. Total bone marrow or fetal liver cells were stained with antibodies to label HSCs and hematopoietic progenitors. After being washed twice with the FACS washing buffer (PBS containing 2% FBS) and once with 1x Annexin V binding buffer (eBioscience), cells were incubated, in dark at room temperature for 15 min, with 1x Annexin V binding buffer containing Annexin V-PECy7 (eBioscience, Table S5). Cells were analyzed with an LSR II flow cytometer (BD Biosciences) within 4 h after staining.

Reactive oxygen species (ROS) detection. Cells were harvested from the bone marrow of control and vKO pups or the fetal livers of control and vKO embryos. After red cells were lysed with an RBC lysis buffer (diluted from a 10x RBC lysis buffer, eBioscience), nucleated cells were stained in dark at 37°C for 30 min with 2 μM 2',7'-dichlorodihydrofluorescein diacetate (H2DCFDA, Invitrogen) diluted from a 2 mM stock with pre-warmed PBS, according to a detailed procedure described in the user's

manual for H2DCFDA (Thermo Scientific). Cells were washed twice in a cold FACS washing buffer and stained with conjugated monoclonal antibodies (Table S5) to label HSCs and hematopoietic progenitors in dark at 4°C for 30 min. Cells were subsequently analyzed with a Fortessa flow cytometer (BD Biosciences).

Cellular senescence determination. Senescence was quantified via a published method (3). Briefly, cells were harvested from wild-type and vKO bone marrows. After lysis of red blood cells, nucleated cells were suspended in 1 ml of the culture medium (DMEM supplemented with 2% FBS and 100 U/ml penicinin and 100 μg/ml streptomycin), and bafilomycin A1 was added to a final concentration of 100 mM. After incubation in a cell culture incubator (5% CO_2 and 37°C) for 1 h, 16.5 μl of 2mM 5-dodecanoylaminofluorescein di-β-D-galactopyranoside (C12FDG, Setareh Biotech; diluted with the culture medium from a 20 mM stock) was added into the cell mixture to a final concentration of 33 μM. After incubation for 30 min, the cell mixture was centrifugated at 500 *g* for 5 min, and the supernatant was aspirated and discarded. The cell pellet was suspended in 1 ml PBS and then centrifugated at 500 *g* for 5 min. This washing step was repeated once and the cells were subsequently stained with FVD506 and fluorophore-conjugated monoclonal antibodies (Table S5) for flow cytometry to assess senescence in HSCs and hematopoietic progenitors.

Bone marrow transplantation. The assays were performed as described (4), with some

modifications. About 8-week old CD45.1$^+$ C57B/L6.SJL recipient mice (Jax) were irradiated at 9 Gy (split into 2 doses of 4.5 Gy, 3 h apart) with an X-ray irradiator (Rad Source, RS-2000). 1x10^6 C57B/L6 control or vKO bone marrow nucleated cells (CD45.2$^+$) were mixed with 1x10^6 CD45.1$^+$ bone marrow nucleated cells (isolated from B6.SJL mice) and injected via tail vein into the lethally irradiated CD45.1$^+$ C57B/L6.SJL recipient mice. Similarly, when fetal liver cells were used as donors, 1x10^6 C57B/L6 control or vKO fetal liver nucleated cells (CD45.2$^+$) were mixed with 1x10^6 CD45.1$^+$ fetal liver nucleated cells (isolated from C57B/L6.SJL mice) and injected via tail vein into the lethally irradiated CD45.1$^+$ C57B/L6.SJL recipient mice. The peripheral blood samples were collected at 4, 8, 12 and 16 weeks after transplantation, and stained with multilineage markers, CD45.1-APCCy7 and CD45.2-Pacific Blue (Table S5) for analysis of the engraftment. The bone marrow was collected at week 16 or 22 for engraftment analysis by multicolor flow cytometry on an LSR II flow cytometer (BD Biosciences) (5, 6). The FACSDiva (BD Biosciences) and FlowJo (TreeStar Inc.) software packages were used for data analysis.

Homing assays. 2x10^6 nucleated bone marrow cells from CD45.2$^+$ control or mutant pups were suspended in 0.9% NaCl and injected via tail vein into X-ray irradiated 8-week old CD45.1$^+$ C57BL/6.SJL recipient mice (see above). 40 h after transplantation, recipient mice were sacrificed and bone marrow cells were collected for analysis by flow cytometry to determine the contribution of CD45.2$^+$ control or mutant donor cells.

RNA-Seq. Fetal livers were dissected from wild-type and vKO embryos at E14.5, homogenized by pipetting and filtered through a 40 μm cell strainer (BD Bioscences) to prepare single-cell suspension. The suspension was centrifugated, and the cell pellet was lysed in an RBC lysis buffer (eBioscience) and stained with fixable viability dye 506 (eBioscience). Cells were subsequently stained for cell surface antigens with a mixture of conjugated antibodies of Lin (CD3e, B220, Gr1, Ter119)-PerCPCy5.5, Sca1-APC and cKit-Pacific Blue (Table S5). After a single wash, LSK cells were sorted on an Aria sorter (BD Biosciences). LSK cells (~10,000) were sorted directly into a collecting tube containing 0.7 ml QIAZOL (Qiagen) and were kept on ice. Four embryos were used to pool sufficient wild-type or mutant LSK cell. The sorted cells were frozen immediately on dry ice and stored at -80°C. The total RNA was isolated by use of the miRNeasy Mini kit (QIAGEN). The yield was determined on a Nanodrop 2000 spectrophotometer (Thermo Scientific) and the integrity was assessed with an RNA Pico chip on an Agilent 2100 Bioanalyzer. Two independent pairs of wild-type and vKO RNA samples (each of which contained LSK cells pooled from four embryos) were used for oligo-dT primed RNA Seq on HiSeq2500 sequencers (Illumina). RNA-Seq was performed in two different companies, Otogenetics and Omega Bioservices. Raw sequencing reads were mapped to the mouse reference genome NCBI37/mm9 via TopHat and differential expression between the wild-type and mutant was calculated by Cufflink. Genes up- and down-regulated in the mutant were subject to gene set

enrichment analysis (GSEA). Interesting candidates were selected for further validation by RT-qPCR.

RT-qPCR. For validation of candidates selected from RNA-Seq and bioinformatic analysis, LSK cells were isolated as described above from wild-type and mutant embryos at E12.5 and E14.5. RNA was reverse-transcribed by the QuantiTect Reverse Transcription kit (QIAGEN). Real-time qPCR was performed on Realplex2 (Eppendorf) with the Green-2-Go qPCR Mastermix (BioBasic). Primer sequences were taken from PrimerBank (http://pga.mgh.harvard.edu/primerbank/) or designed on the web-based IDT RT-qPCR primer designer. Primers were synthesized by IDT Biotechnology, with their sequences listed in Table S6.

Protein extraction and Western blotting. Bone marrow cells were harvested from the femur and tibia, and suspended in DMEM containing 2% FBS. After washing once with PBS, cells were lysed in the RIPA buffer (150 mM NaCl, 1.0% NP-40, 0.5% sodium deoxycholate, 0.1% sodium dodecyl sulfate, 50 mM Tris-HCl pH8.0 and protease inhibitors). After centrifugation at 13,000 *g* and 4°C for 10 min, the supernatant was collected as the soluble protein extract for immunoblotting with anti-histone H3 (Abcam, ab1791), anti-H3K9ac (Abcam, ab10812), anti-H3K14ac (Millipore, 07-353), anti-H3K18ac (Millipore, 07-354), anti-H3K23ac (Millipore, 07-355), anti-histone H4 (Millipore, 05-858) and anti-H4K16ac (Abcam, ab109463)

antibodies.

For analysis of histone acetylation in the kidney, wild-type and mutant pups were sacrificed and kidneys were collected in 1.5 ml Eppendorf tubes and snap-frozen on dry ice. Before tissue homogenization, ~250 μl of the RIPA buffer was added to each frozen kidney and a small pestle was used to crush the tissue manually on ice until no solid tissue was present (~20 times). The mixture was further sonicated on ice. After centrifugation at 13,000 *g* and 4°C for 10 min, the supernatant was used as the soluble extract for immunblotting with the aforementioned antibodies.

Indirect immunofluorescence microscopy. LSK cells from the wild-type or mutant bone marrow at P7 were sorted directly into PBS containing 2% FBS. The cells were spun down immediately onto a glass slide (Fisher Scientific, 12-550-19) at 800 *g* for 6 min on a Cytospin centrifuge (StatSpin CytoFuge 2, Beckman Coulter). After fixation in 2% PFA for 10 min, the cells were subject to indirect immunofluorescence microscopy as described (7, 8). Briefly, the cells were permeabilized in PBS containing 0.2% Triton X-100 for 15 min, blocked in 2% BSA for 30 min, and incubated with primary antibodies (same as those described above for immunoblotting) for 1 h at room temperature. After washing, the cells were incubated with Alexa Fluor-labeled anti-rabbit IgG (Invitrogen, A-11011) for 1 h, and the nuclei were counter-stained with 4',6-diamidino-2-phenylindole (DAPI). The slide was finally mounted with a coverslip by use of Immu-Mount (Thermo Scientific) for examination on an

Axio Observer Z1 fluorescence microscope (Zeiss) controlled by the Zen software package (Zeiss). Images were processed with Adobe Photoshop and Illustrator (Adobe CS6).

Glucose measurement. Serum glucose levels in control and mutant pups were measured at P9 or P11 with an Accu-Check glucose meter (Roche).

SUPPLEMENTAL REFERENCES

1. You L, Zou J, Zhao H, Bertos NR, Park M, Wang E, and Yang XJ. Deficiency of the chromatin regulator Brpf1 causes abnormal brain development. *J Biol Chem.* 2015;290(7114-29.
2. You L, Yan K, Zou J, Zhao H, Bertos NR, Park M, Wang E, and Yang XJ. The lysine acetyltransferase activator Brpf1 governs dentate gyrus development through neural stem cells and progenitors. *PLoS Genet.* 2015;11(e1005034.
3. Debacq-Chainiaux F, Erusalimsky JD, Campisi J, and Toussaint O. Protocols to detect senescence-associated beta-galactosidase (SA-betagal) activity, a biomarker of senescent cells in culture and in vivo. *Nat Protoc.* 2009;4(12):1798-806.
4. Nijnik A, Woodbine L, Marchetti C, Dawson S, Lambe T, Liu C, Rodrigues NP, Crockford TL, Cabuy E, Vindigni A, et al. DNA repair is limiting for haematopoietic stem cells during ageing. *Nature.* 2007;447(7145):686-90.
5. Perfetto SP, Chattopadhyay PK, and Roederer M. Seventeen-colour flow cytometry: unravelling the immune system. *Nat Rev Immunol.* 2004;4(8):648-55.
6. Mayle A, Luo M, Jeong M, and Goodell MA. Flow cytometry analysis of murine hematopoietic stem cells. *Cytometry A.* 2013;83(1):27-37.
7. Walkinshaw DR, Weist R, Kim GW, You L, Xiao L, Nie J, Li CS, Zhao S, Xu M, and Yang XJ. The tumor suppressor kinase LKB1 activates the downstream kinases SIK2 and SIK3 to stimulate nuclear export of class IIa histone deacetylases. *J Biol Chem.* 2013;288(13):9345-62.
8. Walkinshaw DR, Weist R, Xiao L, Yan K, Kim GW, and Yang XJ. Dephosphorylation at a Conserved SP Motif Governs cAMP Sensitivity and Nuclear Localization of Class IIa Histone Deacetylases. *J Biol Chem.* 2013;288(8):5591-605.
9. Cheng CW, Adams GB, Perin L, Wei M, Zhou X, Lam BS, Da Sacco S, Mirisola M, Quinn DI, Dorff TB, et al. Prolonged fasting reduces IGF-1/PKA to promote hematopoietic-stem-cell-based regeneration and reverse immunosuppression. *Cell Stem Cell.* 2014;14(6):810-23.
10. Leung A, Ciau-Uitz A, Pinheiro P, Monteiro R, Zuo J, Vyas P, Patient R, and Porcher C. Uncoupling VEGFA functions in arteriogenesis and hematopoietic stem cell specification. *Dev Cell.* 2013;24(2):144-58.
11. Kobayashi I, Kobayashi-Sun J, Kim AD, Pouget C, Fujita N, Suda T, and Traver D. Jam1a-Jam2a interactions regulate haematopoietic stem cell fate through Notch signalling. *Nature.* 2014;512(7514):319-23.
12. Frelin C, Herrington R, Janmohamed S, Barbara M, Tran G, Paige CJ, Benveniste P, Zuniga-Pflucker JC, Souabni A, Busslinger M, et al. GATA-3 regulates the self-renewal of long-term hematopoietic stem cells. *Nat Immunol.* 2013;14(10):1037-44.
13. Doulatov S, Vo LT, Chou SS, Kim PG, Arora N, Li H, Hadland BK, Bernstein ID, Collins JJ, Zon LI, et al. Induction of multipotential hematopoietic progenitors from human pluripotent stem cells via respecification of lineage-restricted

precursors. *Cell Stem Cell.* 2013;13(4):459-70.
14. Wright DE, Bowman EP, Wagers AJ, Butcher EC, and Weissman IL. Hematopoietic stem cells are uniquely selective in their migratory response to chemokines. *J Exp Med.* 2002;195(9):1145-54.
15. Kiel MJ, Yilmaz OH, Iwashita T, Yilmaz OH, Terhorst C, and Morrison SJ. SLAM family receptors distinguish hematopoietic stem and progenitor cells and reveal endothelial niches for stem cells. *Cell.* 2005;121(7):1109-21.
16. McKinney-Freeman S, Cahan P, Li H, Lacadie SA, Huang HT, Curran M, Loewer S, Naveiras O, Kathrein KL, Konantz M, et al. The transcriptional landscape of hematopoietic stem cell ontogeny. *Cell Stem Cell.* 2012;11(5):701-14.
17. Challen GA, Sun D, Jeong M, Luo M, Jelinek J, Berg JS, Bock C, Vasanthakumar A, Gu H, Xi Y, et al. Dnmt3a is essential for hematopoietic stem cell differentiation. *Nat Genet.* 2011;44(1):23-31.
18. Lam K, and Zhang DE. RUNX1 and RUNX1-ETO: roles in hematopoiesis and leukemogenesis. *Front Biosci (Landmark Ed).* 2012;17(1120-39.
19. Chambers SM, Boles NC, Lin KY, Tierney MP, Bowman TV, Bradfute SB, Chen AJ, Merchant AA, Sirin O, Weksberg DC, et al. Hematopoietic fingerprints: an expression database of stem cells and their progeny. *Cell Stem Cell.* 2007;1(5):578-91.
20. Fu X, and Kamps MP. E2a-Pbx1 induces aberrant expression of tissue-specific and developmentally regulated genes when expressed in NIH 3T3 fibroblasts. *Mol Cell Biol.* 1997;17(3):1503-12.
21. Yan K, You L, Degerny C, Ghorbani M, Liu X, Chen L, Li L, Miao D, and Yang XJ. The chromatin regulator BRPF3 preferentially activates the HBO1 acetyltransferase but is dispensable for mouse development and survival. *J Biol Chem.* 2016;291(2647-63.

Table S1 Offspring genotypes from mating between *Brpf1*$^{f/f}$ and *Brpf1*$^{f/+}$*;Vav1-cre* animals

Day	*Brpf1*$^{f/f}$	*Brpf1*$^{f/+}$	*Brpf1*$^{f/f}$; Vav1-cre	*Brpf1*$^{f/+}$; Vav1-cre	Missing[c]	Total	Chi-test[d]
Birth to P14	102+2[a]+1[b] (26.4%)	96+2[a] (24.6%)	78+2[a] (20.1%)	101+2[a] (25.9%)	12 (3.1%)	398	*
P16-P21	16 (34.0%)	12 (25.5%)	1+5[a] (12.8%)	11 (23.4%)	2 (4.3%)	47	***
E14.5	26 (24.1%)	28 (25.9%)	25 (23.1%)	24 (22.2%)	5 (4.6%)	108	ns
E16.5-17.5	11 (22.4%)	9 (18.4%)	12 (24.5%)	16 (33.3%)	1 (2.0%)	49	ns
Expected ratio	25%	25%	25%	25%		100%	

[a] Pups were dead.

[b] Pups were much smaller than normal.

[c] Missing pups (perhaps due to cannibalism) or embryos (resulting from resorption), leading to the lack of available genotyping data.

[d] *, $p<0.05$, ***, $p<0.001$; ns, not statistically significant.

Table S2 Complete blood counts in control and vKO pups at P17

		Control	vKO
Erythroid	RBCs $x10^{12}$/L	4.73±0.18	0.65±0.03***
	MCV fL	45±1	53±1*
	Hemoglobin g/L	74±2	11±4**
	Hematocrit L/L	0.217±0.010	0.035±0.002***
	MCH pg	15.7±0.3	17.1±7.1
	MCHC g/L	347±5	323±132
Leukocytes	WBCs $x10^9$/L	3.0±0.8	0.6±0.2*
	Neutrophils %	23±12	7±5
	Lymphocytes %	67±12	27±22
	Monocytes %	0±0	0±0
	Eosinophils %	0±0	0±0
Platelets	Platelets $x10^9$/L	449±159	29±14

Note: Values represent mean ± SEM, calculated from 5 wild-type and 3 vKO pups. *, $p<0.05$; **, $p<0.01$; ***, $p<0.001$. Abbreviations: MCH, mean corpuscular hemoglobin (average amount of hemoglobin per red blood cell); MCHC, mean corpuscular hemoglobin concentration; MCV, mean corpuscular volume (average volume of red blood cells); RBC, red blood cell; WBC, white blood cell.

Table S3 Complete blood counts in control and vKO pups at P12

		Control	vKO
Erythroid	RBCs $x10^{12}$/L	4.56±0.20	4.53±1.53
	MCV fL	54±6	57±4
	Hemoglobin g/L	86±13	92±29
	Hematocrit L/L	0.246±0.035	0.262±0.094
	MCH pg	18.9±2.2	20.3±1.1
	MCHC g/L	350±5	353±14
Leukocytes	WBCs $x10^9$/L	3.3±1.0	0.6±0.1**
	Neutrophils %	8±3	nd
	Lymphocytes %	88±5	nd
	Monocytes %	0±1	nd
	Eosinophils %	3±3	nd
Platelets	Platelets $x10^9$/L	632±405	44±4***

Note: Values represent mean ± SEM, calculated from 3 pairs of wild-type and vKO pups. **, $p<0.01$; ***, $p<0.001$. See Table S2 for abbreviations. nd, not detectable.

Table S5 Fluorophore-conjugated monoclonal antibodies used for flow cytometry

Antibody	Company	Cat. No.	Clone	Flurochrome
CD3ε	eBioscience	45-0031-80	145-2C11	PerCPCy5.5
B220	eBioscience	45-0452-80	RA3-6B2	PerCPCy5.5
Gr-1	eBioscience	45-5931-80	RB6-8C5	PerCPCy5.5
Gr-1	eBioscience	12-5931-81	RB6-8C5	PE
Ter119	eBioscience	45-5921-80	Ter119	PerCPCy5.5
Mac-1	eBioscience	45-0112-80	M1/70	PerCPCy5.6
Sca-1	eBioscience	17-5981-81	D7	APC
cKit	eBioscience	25-1171-82	2B8	PECy7
cKit	eBioscience	48-1171-80	2B9	Pacific Blue
CD127(IL-7Rα)	eBioscience	12-1271-81	A7R34	PE
CD135(Flt3)	eBioscience	15-1351-81	A2F10	PE
CD16/32	eBioscience	12-0161-81	93	PE
CD34	eBioscience	11-0341-81	RAM34	FITC
CD150	eBioscience	12-1502-80	mShad150	PE
CD48	eBioscience	11-0481-81	HM48-1	FITC
CD71	eBioscience	12-0711-81	R17217	PE
CD19	eBioscience	12-0193-81	eBio1D3	PE
CD4	eBioscience	12-0041-81	GK1.5	PE
CD8α	eBioscience	11-0081-81	53-6.7	FITC
Ki67	eBioscience	11-5698-82	SolA15	FITC
Annexin V	eBioscience	88-8103-72	/	PECy7
CD45.1	eBioscience	47-0453-82	A20	APCCy7
CD45.2	eBioscience	48-0454-80	104	Pacific Blue

Table S6 Primers for real-time PCR

Gene	Forward Primer	Reverse Primer
Brpf1-f	CAGTAAGATCACCAACCGCC	GAGGAAAGGGGTCAGCTGCA
Brpf1-n	CAGCCCCTCTGAAGTCTCAC	CTAGTGCATTGGGGTCACCT
Moz	ATGGTAAAACTCGCTAACCCG	CGTCCCGTCTTTGACGCTC
Moz m	GTGATATCCAAGAACAAGCACTG	TGAGGGTACGGAGAGGAATAC
Moz c	CCTCGTGCATTGGCTGTTC	TCATGGCATTCAAGGTGTTCAT
Morf	AGAAGAAAAGGGGTCGTAAACG	GTGGGAATGCTTTCCTCAGAA
Hbo1	ATGCCGCGAAGGAAGAGAAAT	TCTTGGGAACTCTGGCTTAGC
Brpf2	AACACTGACCTACGCACAAGC	GCCTCTCGCTGTTCTCCTTATT
Brpf3	ACAAGCTCAAGATGCTAGAAGGC	TAGCTGGAAGTGACAAAGGCA
Myct1	ATGGCTAATAACACCACGAGC	CAGCGCCCAGAGAAATCCT
Ebf1	GCATCCAACGGAGTGGAAG	GATTTCCGCAGGTTAGAAGGC
Lef1	TGTTTATCCCATCACGGGTGG	CATGGAAGTGTCGCCTGACAG
Pax5	CCATCAGGACAGGACATGGAG	GGCAAGTTCCACTATCCTTTGG
Nkx2-3	AAGGGACGCAGTTTTCCGATG	GCAGCAGCTAGTGAGTTCAAATA
Ets1	TCCTATCAGCTCGGAAGAACTC	TCTTGCTTGATGGCAAAGTAGTC
Hlf	GACAGCTCCCCTTGAACCC	CTGCTGCTCTCATCGTCCA
Meis1	GCAAAGTATGCCAGGGGAGTA	TCCTGTGTTAAGAACCGAGGG
Foxa3	GCTGACCCTGAGTGAAATCTAC	ACGAAGCAGTCATTGAAGGAC
Etv1	TTAAGTGCAGGCGTCTTCTTC	GGAGGCCATGAAAAGCCAAA
Amotl1	ATGTAGCCTCTGGAAGAGTGT	TGAGTGAGGGTTTCCGTGGA
Ccr9	TCTGCATTACCATCTGGGTGA	ATTCCCCACTGACTTGACTGT
Cecr2	AGTGATCTGATTGCCTGCTTG	AGCTCCCAACGGTAGTTAATGA
Mecom	AAGTAATGAGTGTGCCTATGGC	AGTTGACTCTCGAAGCTCAAAC
Mecom	TTCCTTCGGGCTTATACCACA	TTTTCTCAAGGGGCCTCTCTT
Sox6	GGTCATGTTTCCCACCCACAA	TTCAGAGGGGTCCAAATTCCT
Slamf1	CAGAAATCAGGGCCTCAAGAG	CACTGGCATAAACTGTGGTGG
Eto	ATGCCTGATCGTACCGAGAAG	GTCGTTGGCGTAAATGAGCTG
Bcl6b	GGCTACGTCCGAGAGTTCAC	CTTGTGCGCTCTTAGGGGT
Bax	TGAAGACAGGGGCCTTTTTG	AATTCGCCGGAGACACTCG
Bst2	TGTTCGGGGTTACCTTAGTCA	GCAGGAGTTTGCCTGTGTCT
Fgf13	CTCATCCGGCAAAAGAGACAA	TTGGAGCCAAAGAGTTTGACC
Gfi1	AGAAGGCGCACAGCTATCAC	GGCTCCATTTTCGACTCGC
Sox17	TTTCCCGAATTCAGCAGCCCGGATGC GGGATA	TTTCCCAAGCTTTCAAATGTCGGGGTAGTTGC
Hemgn	GGAGGCAGACATCACAATGG	CCTTTTGCTCCACGTTCCCTT
Pou2af1	CACCAAGGCCATACCAGGG	GAAGCAGAAACCTCCATGTCA
Hoxa7	GCGCTTTTTAGCAAATATACGGC	GGGATGTTTTGGTCGTAGGAG
Hoxa9	CCCCGACTTCAGTCCTTGC	GATGCACGTAGGGGTGGTG
Hoxa10	CCTGCCGCGAACTCCTTTT	GGCGCTTCATTACGCTTGC
Hoxb5	CCTTCTCGGGGCGTTATCC	CCTGAAGCGGGGTTCCTTG
p16	GGGTTTCGCCCAACGCCCCGA	TGCAGCACCACCAGCGTGTCC
p19	GTTTTCTTGGTGAAGTTCGTGC	TCATCACCTGGTCCAGGATTC
Cdkn2a	CGCAGGTTCTTGGTCACTGT	TGTTCACGAAAGCCAGAGCG
p15	CCCTGCCACCCTTACCAGA	CAGATACCTCGCAATGTCACG
p21	CACAGCGACCATGTCCAA	GCGGGGCTCCCGTGGGCACT
p57	CCAAGCTGGACAGGACAAGC	AGTCCCAGCGGTTCTGGTCC

p27	TGTCAGCGGGAGCCGCCAGG	ATATCTTCCTTGCTTCATAA
Rpls14	TGCCACATCTTTGCATCCTTC	ACTCATCTCGGTCAGCCTTCA
Rps19	CAGCAGGAGTTCGTCAGAGC	CACCCATTCGGGGACTTTCA
Rpl13	AGCCGGAATGGCATGATACTG	TATCTCACTGTAGGGCACCTC
Rpl26	ACTTCTGACCGAAGCAAGAAC	CCGAATGGGCATAGACCGAA
Rpl41	CATCTTCCTTGAGACTCCTGC	CATCCCTCACTTCTGCTCC
Rpl38	GAAGTTCAAGGTTCGCTGC	TTTAATAGTCACACGCAGAGGG
Gapdh	TGATGACATCAAGAAGGTGGTGAA	TCTTACTCCTTGGAGGCCATGT

SUPPLEMENTAL FIGURE LEGENDS

Figure S1. *Brpf1* expression in different hematopoietic lineages from the neonatal bone marrow and fetal liver. (**A**) Relative *Brpf1* mRNA level in LSK, MP ($Lin^-Sca1^-cKit^+$), erythroid cells and other differentiated hematopoietic cells. (**B**) Relative *Brpf1* transcript level in LT-HSC ($Lin^-Sca1^+cKit^+CD34^-Flt3^-$), ST-HSC ($Lin^-Sca1^+cKit^+CD34^+Flt3^-$), GMP ($Lin^-Sca1^-cKit^+CD34^+CD16/32^+$), CMP ($Lin^-Sca1^-cKit^+CD34^+CD16/32^-$) and MEP ($Lin^-Sca1^-cKit^+CD34^-CD16/32^-$) cells. (**C**) Relative *Brpf1* mRNA level in different hematopoietic cell types. Note that the *Brpf1* mRNA level is robust in HSCs ($CD48^-CD150^+$LSK) when compared to other cell types in the hematopoietic system. HPC1, $CD48^+CD150^-$ LSK; HPC2, $CD48^+CD150^+$ LSK; MPP, $CD48^-CD150^-$ LSK; MP, $Lin^-Sca1^-cKit^+$. Cells in (A-B) were sorted from the wild-type bone marrow at P11, and those in (C) were from the wild-type fetal liver at E12.5. For (A), cells were sorted into TRIzol or QIAzol directly and RNA was isolated by use of an RNeasy mini kit for cDNA preparation with a QuantiTect Reverse Transcription kit. For (B) and (C), cells were sorted into a lysis buffer from an ExCellenCT Lysis kit (ABM Inc, G916) and cDNA was prepared directly with the same kit. The mRNA levels were determined by RT-qPCR. In (C), mean values are shown for each population, with the average value of the $Ter119^-CD71^-$ population arbitrarily set to 1.0. n=3 for each cell population in (A-C). For statistical analysis, unpaired 2-tailed Student's *t* tests were performed and the average values are presented as mean ± SEM.

Figure S2. Specific *Brpf1* inactivation in the mutant bone marrow and fetal liver. (**A**) *Brpf1* mRNA level in the bone marrow and testis of control and vKO pups at P7. (**B**) *Brpf1* transcript level in the bone marrow, spleen, thymus and kidney of control and vKO pups at P11. The mRNA level in the mutant kidney was decreased to ~60% of that in the control; the decrease was perhaps due to contribution of various blood cells in the kidney, which is highly vascular and contains lots of such cells. For RNA extraction, fresh tissues were homogenized in TRIzol with a 5/8-inch 25G needle (BD Biosciences, 309626). RNA was extracted via the TRIzol reagent. The RNA levels were determined by RT-qPCR. n=3 for both control and vKO pups (A-B). (**C**) The *Brpf1* mRNA level dramatically decreased in differentiated cells of the mutant bone marrow at P7. Different populations from wild-type and mutant bone marrows were sorted into the TRIzol or QIAzol reagent directly. RNA was extracted with a miRNeasy mini kit. HSCs and hematopoietic progenitors are low in the mutant bone marrow at this stage (Figure 3), so only differentiated cells were analyzed. **(D)** The *Brpf1* mRNA level was dramatically decreased in various hematopoietic populations in the mutant fetal liver at E12.5. Cells were sorted from the wild-type and mutant fetal livers to the TRIzol or QIAzol reagent directly. RNA was extracted with an RNeasy mini Kit and reversely transcribed to cDNA with a QuantiTech Reverse Transcription kit. The mRNA level was determined by RT-qPCR. n=3 for each tissue or cell population, and the average values are presented as mean ± SEM. *, $p<0.05$, **, $p<0.01$, ***, $p<0.001$. For statistical analysis, unpaired 2-tailed Student's *t* tests were

performed and the average values are presented as mean ± SEM.

Figure S3. Comparison of cellularity, B lymphocytes, myeloid cells and erythrocytes in the control and mutant bone marrows. (**A**) Total bone marrow (BM) cells are compared between wild-type and mutant mice at P6. n=5 for each group of pups. **(B**) Comparison of viable bone marrow cells in control and mutant mice at P6. n=5 for each group. (**C-D**) Bone marrow cells from P6 control and mutant pups were stained with Gr1-PerCPCy5.5 and CD19-PE for flow cytometry. $CD19^+$ and $Gr1^+$ populations are demarcated to mark the B and myeloid lineages, respectively. Representative flow cytometric analysis is presented in (C) and the average values are shown in (D). n=5 for control and n=4 for vKO mice. (**E-F**) Same as (C-D) except that Mac1-PerCPCy5.5 and Gr1-PE were used for flow cytometry. n=5 for each group of mice. (**G-H**) Same as (C-D) except that Ter119-PerCPCy5.5 and CD71-PE were used. n=5 for each group. *, $p<0.05$; **, $p<0.01$. For statistical analysis, unpaired 2-tailed Student's *t* tests were performed and the average values are presented as mean + SEM in (A-B), (D), (F) and (H).

Figure S4 *Brpf1* inactivation reduces HSC and progenitor populations in the spleen. (**A-B**) The spleen weight was similar between control and mutant pups at P6 (A, left), whereas total cellularity decreased significantly in the mutant (A, right). Spleen cells were isolated at P6 and stained with PerCPCy5.5-conjugated monoclonal

antibodies specific to the B cell marker B220 or the T cell marker CD3ε, respectively. Total viable cells decreased in the mutant spleen (B, left), but no significant changes were observed with either viable B or T cells (B, right). n=5 for each group of pups. (**C**) Spleen cells were isolated at P6 and stained with PerCPCy5.5-conjugated monoclonal antibodies against four lineage markers (CD3ε, B220, Gr1 and Ter119) and three fluorophore-conjugated monoclonal antibodies specific to HSC markers (Sca1-APC, cKit-Pacific blue and CD150-PE). Populations of LSK cells and hematopoietic progenitors (HPC, $CD150^{+}LSK^{+}$) in total spleen cells are boxed, with the percentage values indicated. n=3 for each group of pups. (**D-E**) In severe cases, small and pallor spleens were found in vKO pups at P6. Representative HE-stained images are presented in (D), with magnified images shown in (E). Note that the white pulps are disorganized or missing in the vKO spleen. Similar results were observed in three pairs of control and mutant pups. For statistical analysis, unpaired 2-tailed Student's *t* tests were performed and the average values are presented as mean + SEM in (A-B). Scale bars, 500 μm (D) and 100 μm (E).

Figure S5. Decreased production but normal differentiation of T cells in the mutant thymus. (**A**) The vKO thymus was smaller than the control at P5. One representative pair was shown. Scale bar, 5 mm. (**B**) The total cellularity was lower in the mutant thymus than the control at P5. n=5 for both control and vKO pups. **, p=0.004. (**C**) Representative cytometric analysis after staining with fluorophore-

conjugated monoclonal antibodies against CD4 and CD8a (CD4-PE and CD8a-FITC). (**D**) Four different fractions of thymocytes are compared. Average values of 5 pairs are shown as mean + SEM. Distribution of four thymocyte populations in the mutant thymus was comparable to that in the control at P5. (**E**) Real-time qPCR analysis of cell cycle inhibitor genes and *Brpf1* in 3 pairs of control and vKO thymi at P7. For statistical analysis, unpaired 2-tailed Student's *t* tests were performed, and average values are shown as mean + SEM in (B) and (D), or as mean ± SEM in (E).

Figure S6. Normal homing of mutant bone marrow stem cells. (**A**) Representative cytometric analysis of $CD45.2^+$ donor cells in the bone marrow $CD45.1^+$ recipients' bone marrow 40 h after transplantation. (**B**) Number of $CD45.2^+$ donor cells in 150,000 total bone marrow nucleated cells as detected in (A). $2x10^6$ nucleated bone marrow cells from control or mutant $CD45.2^+$ C57B/L6 pups at P7 were suspended in 0.9% NaCl and injected via tail vein into lethally irradiated $CD45.1^+$ C57BL/6.SJL recipient mice. n=5 for control and n=6 for vKO donor pups or recipient mice, with cells from one donor injected into one recipient. For statistical analysis, unpaired 2-tailed Student's *t* tests were performed, and average values are shown as mean + SEM in (B). ns, not statistically significant.

Figure S7. **Normal cell cycle progression in mutant fetal liver LSKs at E14.5.** (**A**) Representative cell cycle profiles, with percentage values in each phase of the cell

cycle labeled. Fetal liver cells, isolated from the wild-type, heterozygous and homozygous mutant embryos, were stained with Hochest 33342 and fluorophore-conjugated monoclonal antibodies to gate LSK populations for cell cycle analysis. (**B**) Quantification of the wild-type, heterozygous and homozygous mutant LSK cells in phases of subG1, G1, S, and G2-M of the cell cycle. n=11 for the wild-type (WT), n=6 for heterozygotes and n=4 for homozygous mutants. For statistical analysis, one-way ANOVA was used for multiple comparisons, and average values are shown as mean + SEM. ns, not statistically significant.

Figure S8. Increased ROS and senescence in LSKs but not myeloid progenitors in the mutant neonatal bone marrow. (**A**) Representative cytometric analysis of ROS positive cells in the LSK population. H2DCFDA, 2',7'-dichlorodihydrofluorescein diacetate. (**B**) Representative cytometric analysis of senescent (i.e. SA-β-galactosidase positive) cells in LSK. C12FDG, 5-dodecanoylaminofluorescein di-β-D-galactopyranoside. Experiments in (A-B) were repeated three times and the average values are presented in Figure 7D-E. (**C**) Percentage of ROS positive cells in LSK, $CD150^{+}$LSK, $CD150^{-}$LSK and MP populations in the control and mutant fetal livers at E14.5. n=5 for control or vKO pups. For statistical analysis, unpaired 2-tailed Student's *t* tests were performed, and average values are shown as mean ± SEM in (C). *, $p<0.05$; ns, not statistically significant.

Figure S9. **Reduced transcription of known and potential HSC and progenitor signature genes.** As in Table 1, wild-type and mutant LSK cells were prepared from E14.5 fetal livers for RNA isolation and RNA-Seq. Selected multipotency genes with reduced expression in two different RNA-Seq experiments were used for validation by RT-qPCR with RNA isolated from wild-type and mutant LSK cells sorted from E12.5 and 14.5 fetal livers. The values are shown as fold of change in the mutant compared to the control. For each gene, the two slash-separated numbers in the "RNA-Seq" column represent fold of change in two different RNA-Seq experiments. Genes involved in IGF and Notch signaling are highlighted in light blue and green, respectively; the letters "nd" denote "no detectable expression in the mutant" and the question mark represents "to be determined". Besides those papers described in the main text, additional publications support the known or potential roles for some of the listed genes in HSC homeostasis. For example, IGF1 signaling promotes HSC expansion (9), whereas VEGFA and Notch signaling pathways are important for HSC specification (10, 11). *Gata3* is important for HSC self-renewal (12). *Hoxa9*, *Rora* and *Egr* are able to confer self-renewal and multilineage potential to myeloid precursors *in vitro* (13). *Foxa3*, *Ccr9* and *Vwf* are specifically expressed in HSCs (14-16). Both *Vwf* and *Vldlr* have been considered as HSC fingerprint genes (17). Moreover, some of the listed genes have known or potential roles in the hematopoietic system. For example, *Runx1t1*, formerly known as *Eto*, is a frequent target of acute myeloid leukemia (18). *Fgf13* is highly expressed in lymphoid lineages (19). *Oit3* (oncogene-induced

transcript 3) encodes a poorly characterized protein formerly known as EF9, which was identified as a target of the leukemic protein E2A-PBX1 (20).

Figure S10. Effects on expression of *Brpf1* and related genes in HSCs at E12.5. (**A**) Relative transcript level of *Brpf1*, *Brpf2* and genes for three interacting histone acetyltransferases in HSCs ($CD48^{-}CD150^{+}$LSK) from control and mutant fetal livers at E12.5. The *Brpf1* mRNA level was significantly decreased, but mRNA levels of *Brpf2*, *Moz*, *Morf* and *Hbo1* were not affected in mutant HSCs. We did not assess *Brpf3* because it is non-essential for mouse survival (21). (**B**) Relative expression of *Brpf1, Brpf2* and three interacting histone acetyltransferases in wild-type HSCs at E12.5. Average values are shown for each population in (B), with the average value of the *Morf* mRNA level arbitrarily set to 1.0. Experiments in (A-B) were performed with three pairs of control and mutant animals. For statistical analysis, unpaired 2-tailed Student's *t* tests were performed, and average values are shown here as mean ± SEM. ns, not statistically significant.

Figure S11. Diminished histone H3K23 acetylation in the mutant bone marrow. Immunofluorescence staining with antibodies against histone H3 and its acetylation at lysine 23 (i.e. H3K23ac) in control and mutant bone sections at P5. H3K23 acetylation was low in the mutant bone marrow. Experiments were repeated three times and representative images are shown, with squared regions enlarged in insets. Dashed lines

are used to demarcate the boundary between the bone and marrow regions. Scale bar, 50 μm.

Figure S12. Normal blood glucose levels in mutant pups. Without fasting, control and mutant pups at P9 or P11 were used for determination of glucose levels in tail bloods with a glucose meter (Roche). For the male groups, n=7 for control pups and n=6 for vKO pups; for the female groups, n=5 for both control and vKO pups. For statistical analysis, unpaired 2-tailed Student's *t* tests were performed, and average values are shown here as mean ± SEM. ns, not statistically significant.

Figure S1

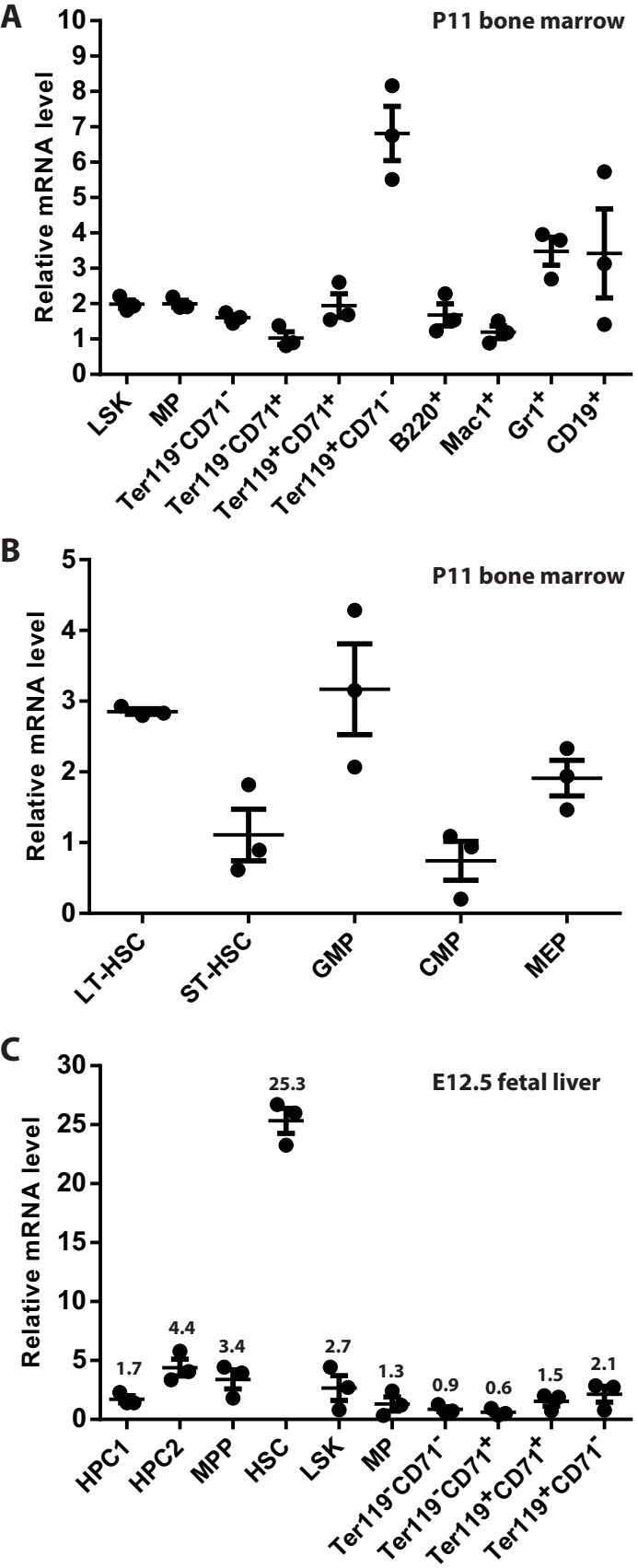
A
P11 bone marrow
Relative mRNA level
10
9
8
7
6
5
4
3
2
1
0
LSK
MP
Ter119-CD71-
Ter119-CD71+
Ter119+CD71+
Ter119+CD71-
B220+
Mac1+
Gr1+
CD19+
B
P11 bone marrow
Relative mRNA level
5
4
3
2
1
0
LT-HSC
ST-HSC
GMP
CMP
MEP
C
E12.5 fetal liver
Relative mRNA level
30
25
20
15
10
5
0
25.3
4.4
3.4
2.7
1.3
0.9
0.6
1.5
2.1
1.7
HPC1
HPC2
MPP
HSC
LSK
MP
Ter119-CD71-
Ter119-CD71+
Ter119+CD71+
Ter119+CD71-

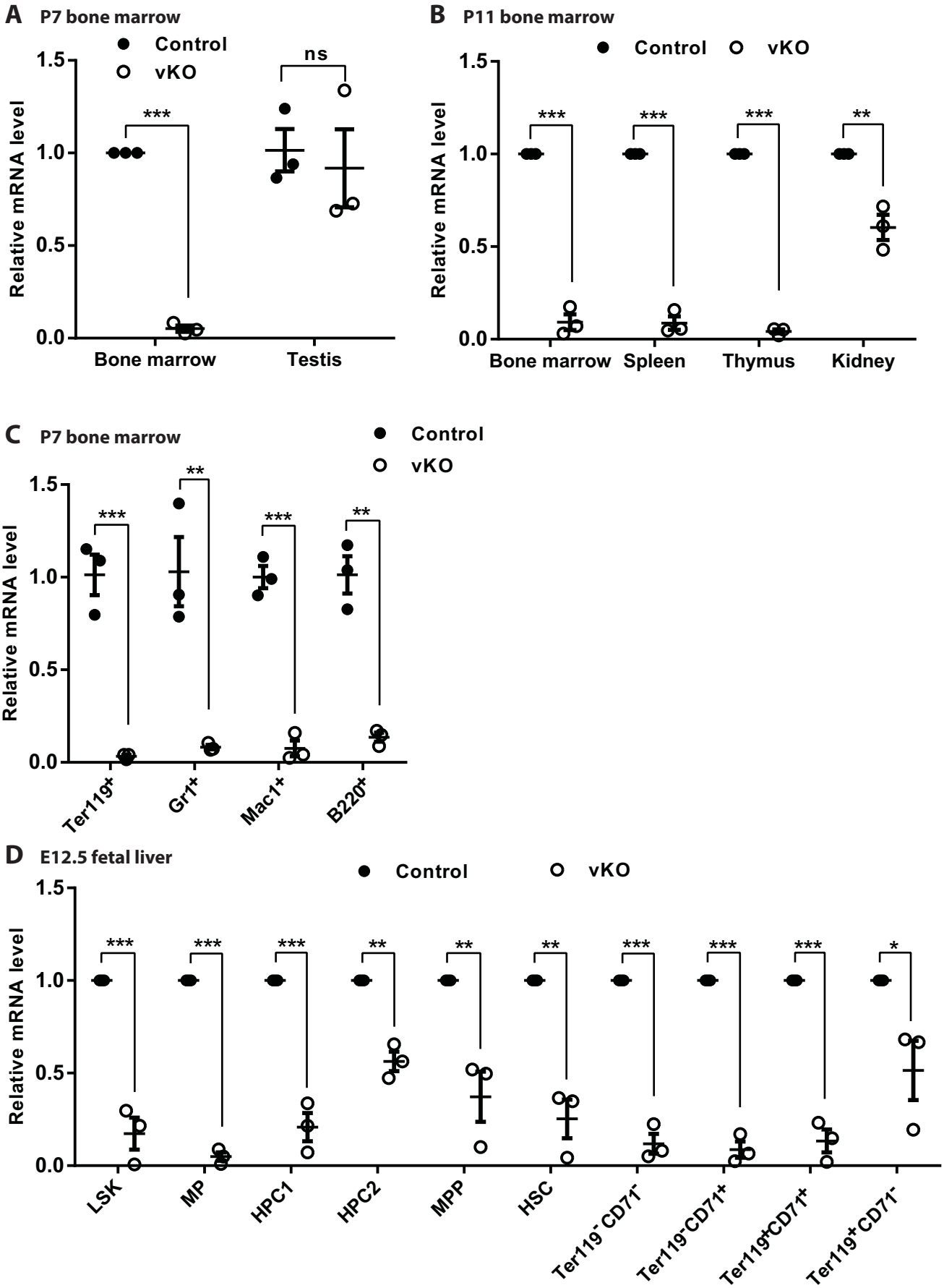
A
P7 bone marrow
Control
vKO
ns
***
Relative mRNA level
1.5
1.0
0.5
0.0
Bone marrow
Testis
B
P11 bone marrow
Control
vKO
***
***
***
**
Relative mRNA level
Bone marrow
Spleen
Thymus
Kidney
C
P7 bone marrow
Control
vKO
***
**
***
**
Relative mRNA level
Ter119+
Gr1+
Mac1+
B220+
D
E12.5 fetal liver
Control
vKO
***
***
***
**
**
**
***
***
***
*
Relative mRNA level
LSK
MP
HPC1
HPC2
MPP
HSC
Ter119-CD71-
Ter119-CD71+
Ter119+CD71+
Ter119+CD71-

Figure S3

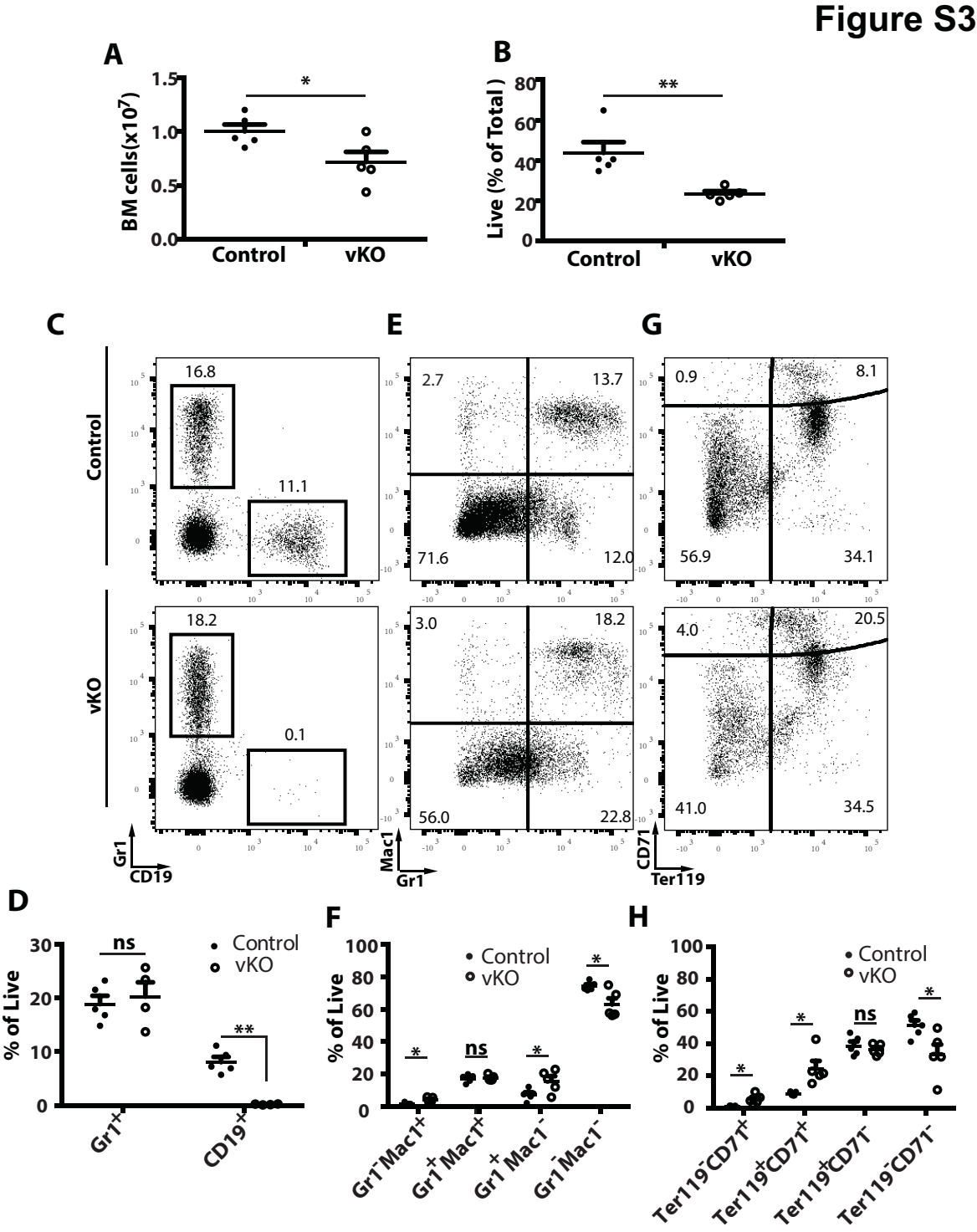
A
BM cells(x10^7)
1.5
1.0
0.5
0.0
*
Control
vKO
B
Live (% of Total)
80
60
40
20
0
**
Control
vKO
C
E
G
Control
vKO
16.8
11.1
18.2
0.1
2.7
13.7
71.6
12.0
3.0
18.2
56.0
22.8
0.9
8.1
56.9
34.1
4.0
20.5
41.0
34.5
Gr1
CD19
Mac1
Gr1
CD71
Ter119
D
% of Live
30
20
10
0
ns
**
Control
vKO
Gr1+
CD19+
F
% of Live
100
80
60
40
20
0
*
ns
*
*
Control
vKO
Gr1-Mac1+
Gr1+Mac1+
Gr1+Mac1-
Gr1-Mac1-
H
% of Live
100
80
60
40
20
0
*
*
ns
*
Control
vKO
Ter119-CD71+
Ter119+CD71+
Ter119+CD71-
Ter119-CD71-

Figure S4

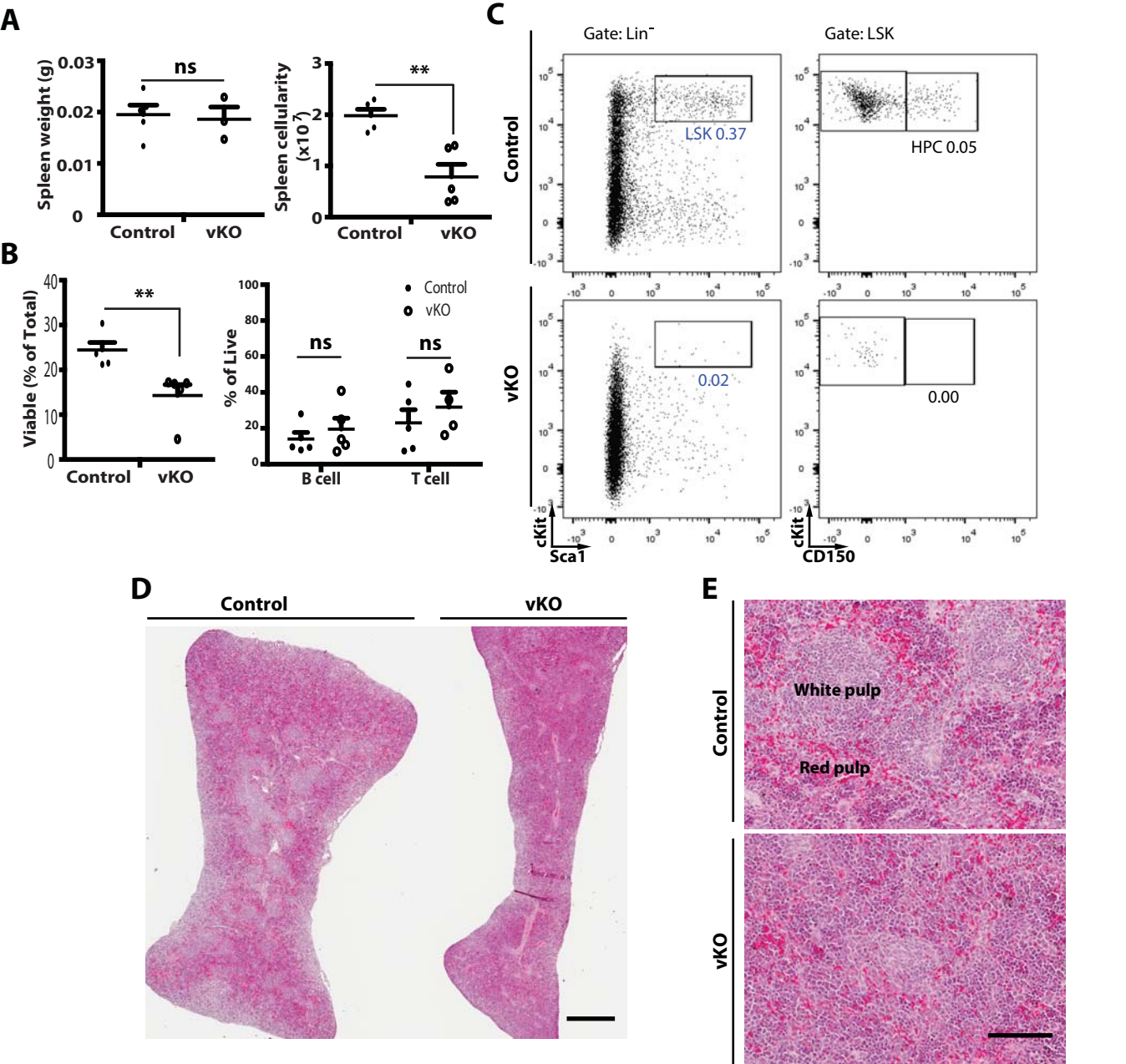
A
Spleen weight (g)
0.03
0.02
0.01
0
ns
Control
vKO
Spleen cellularity (x10^7)
3
2
1
0
**
Control
vKO
B
Viable (% of Total)
40
30
20
10
0
**
Control
vKO
% of Live
100
80
60
40
20
0
Control
vKO
ns
ns
B cell
T cell
C
Gate: Lin-
Gate: LSK
Control
vKO
LSK 0.37
HPC 0.05
0.02
0.00
cKit
Sca1
cKit
CD150
D
Control
vKO
E
Control
vKO
White pulp
Red pulp

Figure S5

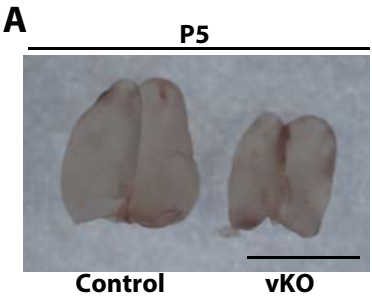

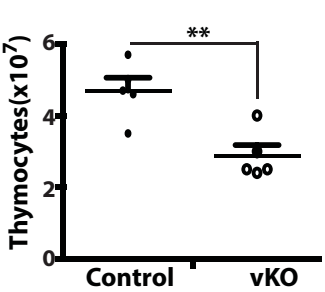

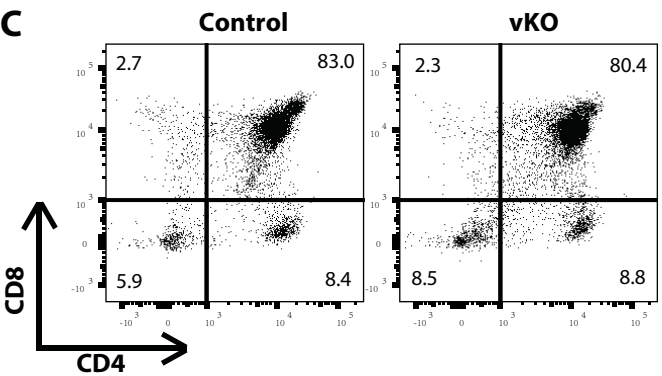

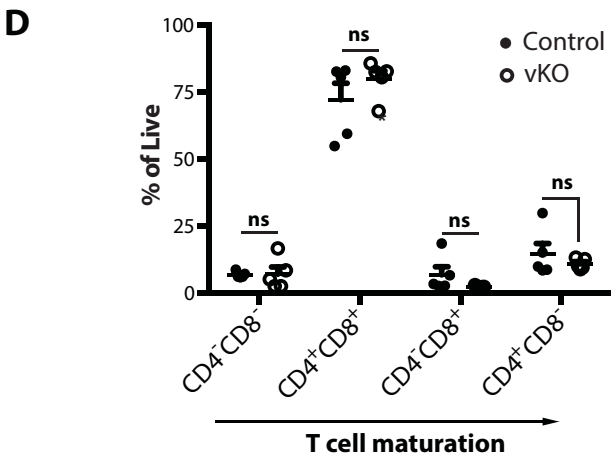

E

Expression of cell cycle inhibitors in the mutant thymus

Gene	Transcript (fold)	*p* value
p16	1.36±0.18	ns
p19	10.89±0.58	<0.001
p21	0.74±0.16	ns
p57	0.52±0.03	<0.01
p27	1.24±0.33	ns
p15	3.40±0.82	<0.05
Brpf1	0.06±0.01	<0.001

Figure S6

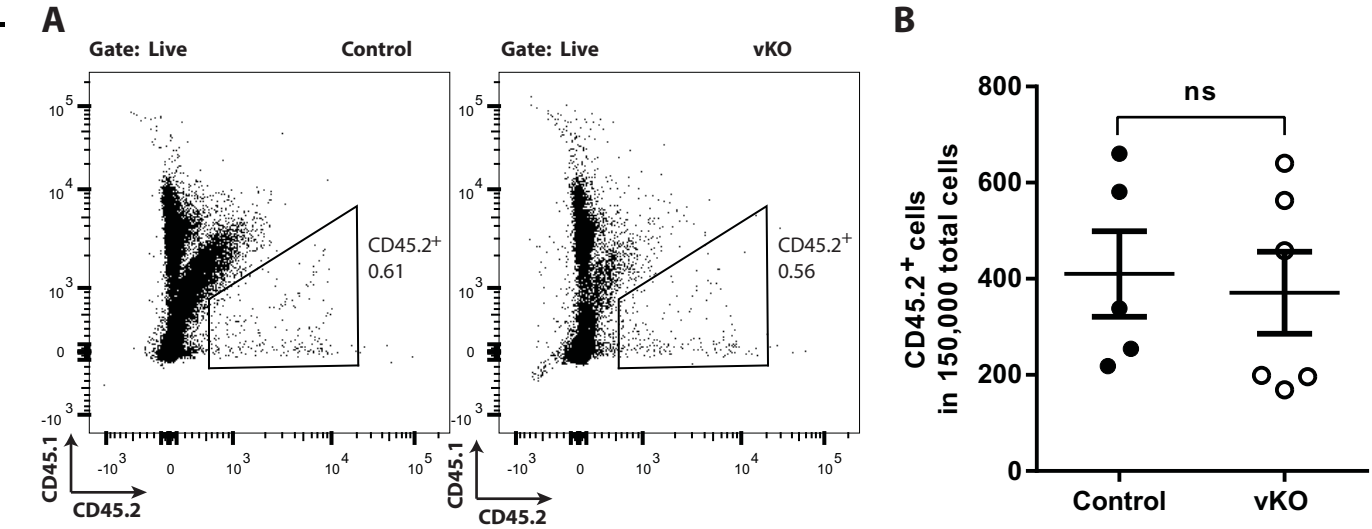
A
Gate: Live
Control
CD45.2+
0.61
CD45.1
CD45.2
Gate: Live
vKO
CD45.2+
0.56
CD45.1
CD45.2
B
ns
CD45.2+ cells
in 150,000 total cells
800
600
400
200
0
Control
vKO

Figure S7

A

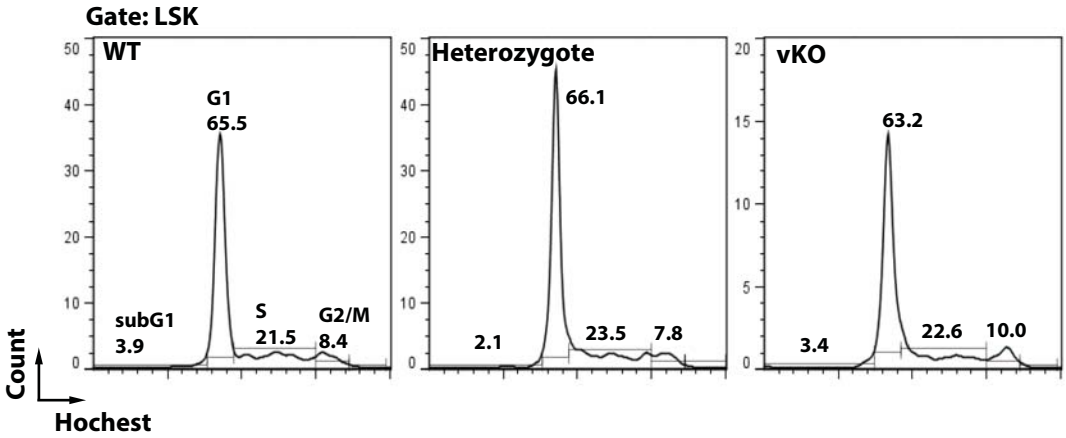
Gate: LSK
WT
G1
65.5
subG1
3.9
S
21.5
G2/M
8.4
Heterozygote
66.1
2.1
23.5
7.8
vKO
63.2
3.4
22.6
10.0
Count
Hochest

B

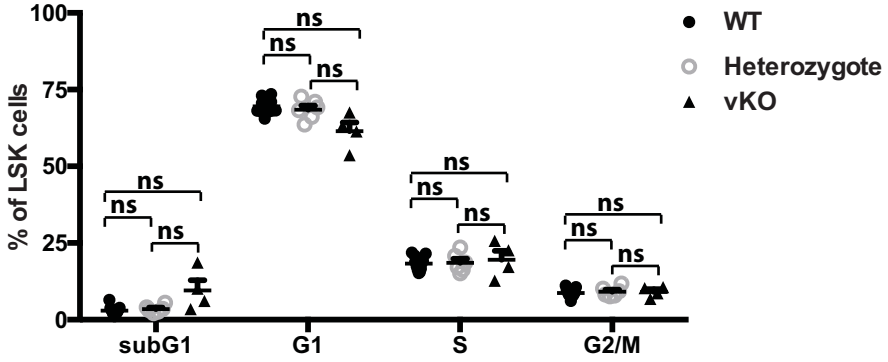
% of LSK cells
100
75
50
25
0
ns
subG1
G1
S
G2/M
WT
Heterozygote
vKO

Figure S8

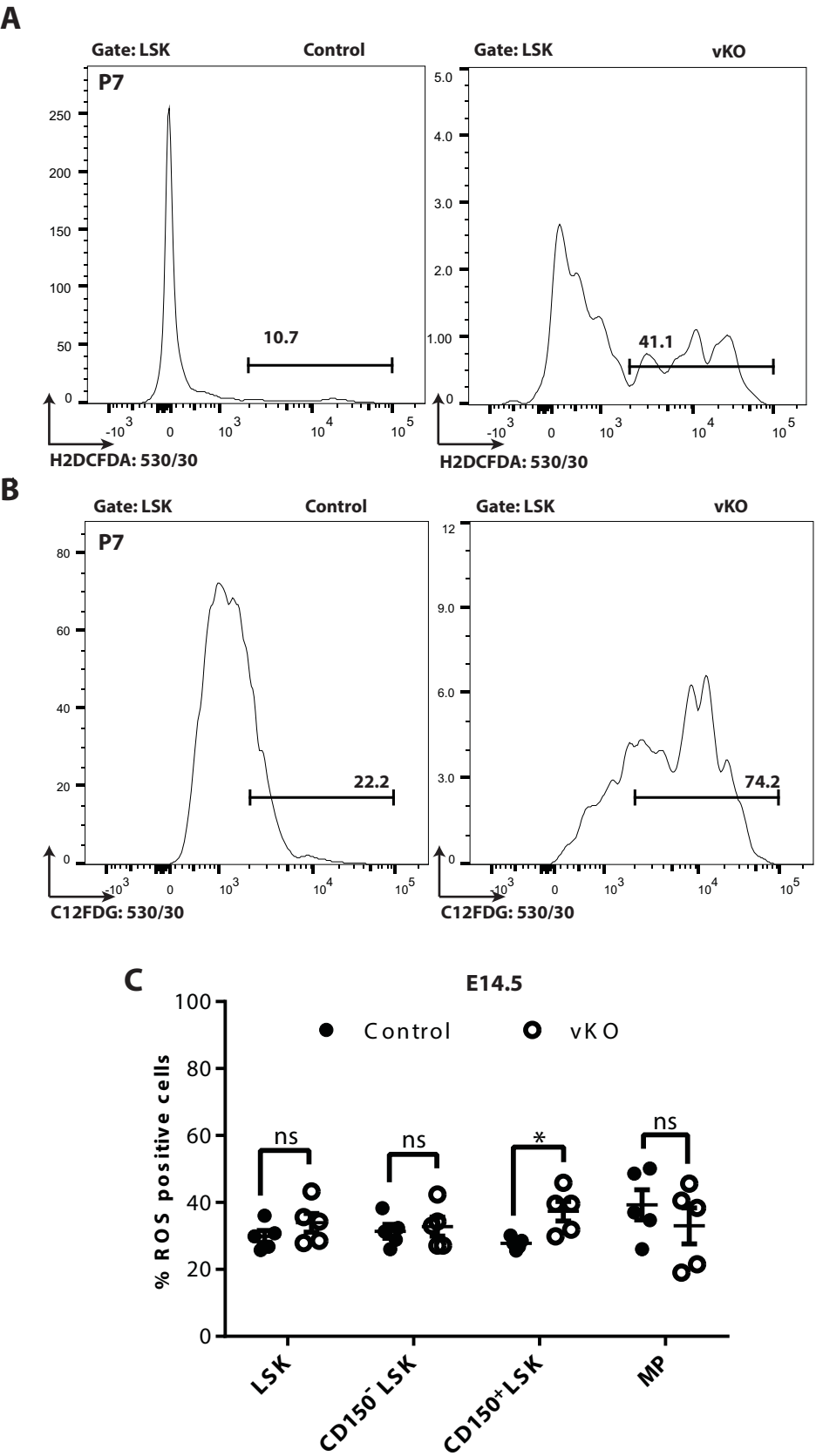
A
Gate: LSK
Control
P7
10.7
H2DCFDA: 530/30
Gate: LSK
vKO
41.1
H2DCFDA: 530/30
B
Gate: LSK
Control
P7
22.2
C12FDG: 530/30
Gate: LSK
vKO
74.2
C12FDG: 530/30
C
E14.5
Control
vKO
% ROS positive cells
ns
ns
*
ns
LSK
CD150⁻ LSK
CD150⁺LSK
MP

Figure S9

Reduced transcription of known and potential HSC and progenitor signature genes

Gene	RNA-Seq (-fold)	RT-qPCR (-fold)		
	E14.5	E14.5	E12.5	
Lef1	0.015/nd	nd	nd	
Pou2af1	0.017/0.035	nd	nd	
Ebf1	0.022/0.071	0.050	0.050	
Sox6	0.055/0.526	1.111	nd	
Fgf13	0.069/0.147	nd	nd	
Ccr9	0.082/0.172	0.178	0.141	
Foxa3	0.110/0.312	0.909	0.110	
Nr2f2	0.133/0.232	?	?	
Igf1	0.172/0.285	?	?	IGF signaling
Hes1	0.185/0.312	?	?	Notch signaling
Nk2-3	0.196/0.333	0.385	0.303	
Notch3	0.222/0.357	?	?	Notch signaling
IL7R	0.238/0.285	?	?	
Igfbp1	0.270/0.555	?	?	IGF signaling
Foxo1	0.312/0.345	?	?	IGF signaling
Hnf4a	0.322/0.345	?	?	
Hoxb3	0.333/0.333	?		
Eya1	0.357/0.588	?	?	
Vwf	0.370/0.384	?	?	
Meis1	0.370/0.400	0.667	0.357	
Cdkn1c/p57	0.454/0.588	?	?	
Igf2	0.500/0.500	?	?	IGF signaling
Maml2	0.526/0.714	?	?	Notch signaling

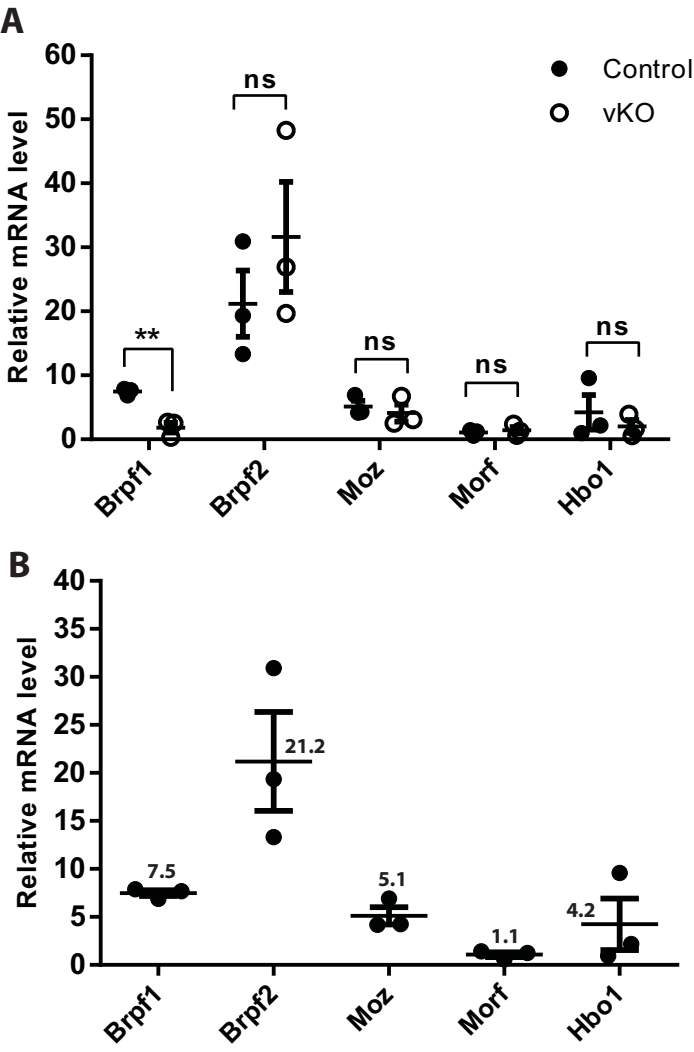
A
Relative mRNA level
60
50
40
30
20
10
0
Control
vKO
**
ns
ns
ns
ns
Brpf1
Brpf2
Moz
Morf
Hbo1
B
Relative mRNA level
40
35
30
25
20
15
10
5
0
21.2
7.5
5.1
1.1
4.2
Brpf1
Brpf2
Moz
Morf
Hbo1

Figure S11

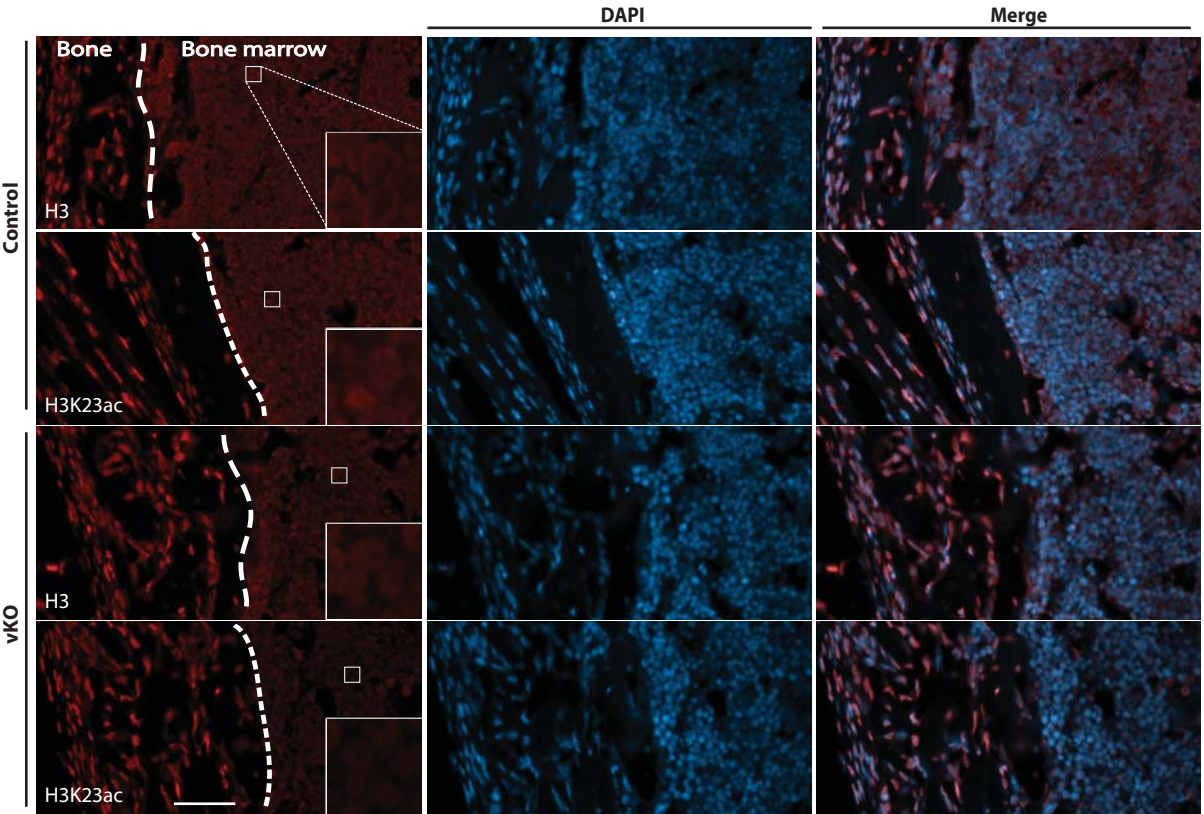
DAPI
Merge
Bone
Bone marrow
H3
H3K23ac
H3
H3K23ac
Control
vKO

Figure S12